

Ionization Spectroscopy of Conformational Isomers of Propanal: The Origin of the Conformational Preference

Sunyoung Choi, Tae Yeon Kang, Kyo-Won Choi, Songhee Han, Doo-Sik Ahn, Sun Jong Baek, and Sang Kyu Kim*

Department of Chemistry and School of Molecular Science (BK21), KAIST, Daejeon (301-750), Republic of Korea

Received: January 26, 2008; Revised Manuscript Received: March 18, 2008

Two different conformational isomers of propanal, *cis* and *gauche*, are investigated by the vacuum-UV mass-analyzed threshold ionization (VUV-MATI) spectroscopy to give accurate adiabatic ionization potentials of 9.9997 ± 0.0006 eV and 9.9516 ± 0.0006 eV, respectively. *cis*-Propanal, which is the more stable conformer in the neutral state, becomes less stable in the cation compared to *gauche*-propanal. Vibrational structures revealed in the MATI spectra indicate that *cis* and *gauche* isomers undergo their unique structural changes upon ionization. The ionization of *gauche*-propanal induces a geometrical change along the conformational coordinate, suggesting that the steric effect in the ground state is diminished upon ionization. Natural bonding orbital (NBO) calculations provide the extent of hyperconjugation in each conformational isomer of propanal.

I. Introduction

Conformational isomers are identified when the internal rotation about the single bond of the molecule gives rise to at least a double-well potential along the rotating angle. Since the barrier height for the internal rotation about the single bond is very low in general, conformational isomers are hardly isolated at ambient conditions. Therefore, it has been nontrivial to extract the conformer-specific information of chemical reactivity, although the structure-based chemistry is ubiquitous in chemistry^{1,2} and biology.^{3,4} Accordingly, the conformer specificity has often been conjectured in the explanation of many important chemical reactions. Supersonic jet spectroscopy provides a great opportunity for the investigation of the conformer-specificity in chemical reactions in this sense. Recently, the conformer-specific chemical reactivity has been unambiguously demonstrated for the photodissociation of 1-iodopropane ion⁵ and propanal ion⁶ or the decarboxylation reaction of alanine and β -alanine ions.⁷ The selection of a specific conformational isomer may be thus utilized as a tool for reaction control. Distinct spectroscopic properties of different conformers such as vibrational frequencies, excited electronic energy, and ionization potential (IP) are therefore quite essential in understanding the conformational preference and studying the conformer-specific chemical reaction dynamics.

Here, we present the ionization spectroscopic result for two conformational isomers of propanal. Propanal is a particularly interesting molecule since its two isomers, *cis* and *gauche*, have been recently reported as showing conformer-specific chemical reactivity in the photodissociation reaction of the molecular cation.⁶ The Suits group, using the photoelectron imaging technique, has reported the IP value of each conformer of propanal with some vibrational features associated with the ionization of each conformer.⁸ In this work, we performed vacuum-UV mass-analyzed threshold ionization (VUV-MATI) spectroscopy of *cis* and *gauche* conformers of propanal. In this way, IP is very accurately determined with much less uncertain-

ties. Moreover, since each conformer is directly ionized by the VUV laser pulse, the structural change that each conformer undergoes upon ionization has been clearly revealed in the high-resolution MATI spectra of *cis* and *gauche* propanals. The experimental results along with theoretical calculations provide insight into the origin of the conformational preference of the propanal molecule.

II. Experimental Section

Propanal (Aldrich) was purchased and used without further purification. The details of the experimental setup have been described in our previous reports.^{9,10} Briefly, the sample at room temperature is mixed with He or Ar carrier gas, expanded into a vacuum through a nozzle orifice (general valve, 0.3 mm diameter) with a backing pressure of 1–3 atm, and skimmed through a 1 mm diameter skimmer (Precision Instrument Services), which is located ~ 10 cm away from the nozzle end. The vacuum chamber was equipped with two turbo pumps to maintain the background pressure of 10^{-7} Torr when the nozzle was operated at 10 Hz. A tunable vacuum UV laser pulse was generated via the four-wave mixing of the UV pulse at 212.552 nm for the $5p[1/2]_0-4p^6$ transition of Kr and VIS laser pulse in a Kr gas cell. The third harmonic output of the Nd:YAG laser (Continuum, Precision 2) was used to pump two independently tunable dye lasers (Scanmate 2 and Lumonics) to generate UV and VIS laser pulses for the VUV laser pulse. The frequency of the VIS laser pulse was calibrated using a wavemeter (Coherent, 33–2619) within an accuracy of 0.5 cm⁻¹.

The VUV laser pulse was collinearly overlapped with the molecular beam in a counter-propagation way to excite the molecule to high-*n* Rydberg states. After a delay time of ~ 10 μ s, the long-lived high-*n*,*l* Rydberg states were pulsed-field ionized using a small electric pulse of ~ 10 V/cm. No spoil field was necessary because of the long delay time between the laser excitation and pulsed-field ionization. Resultant MATI ions were separated according to their mass/charge ratios in the time-of-flight tube prior to being detected by a multichannel plate. The ion signal digitized via an oscilloscope (LeCroy, LT584M) was

* Corresponding author. Fax: +82-42-869-2810. E-mail: sangkyukim@kaist.ac.kr.

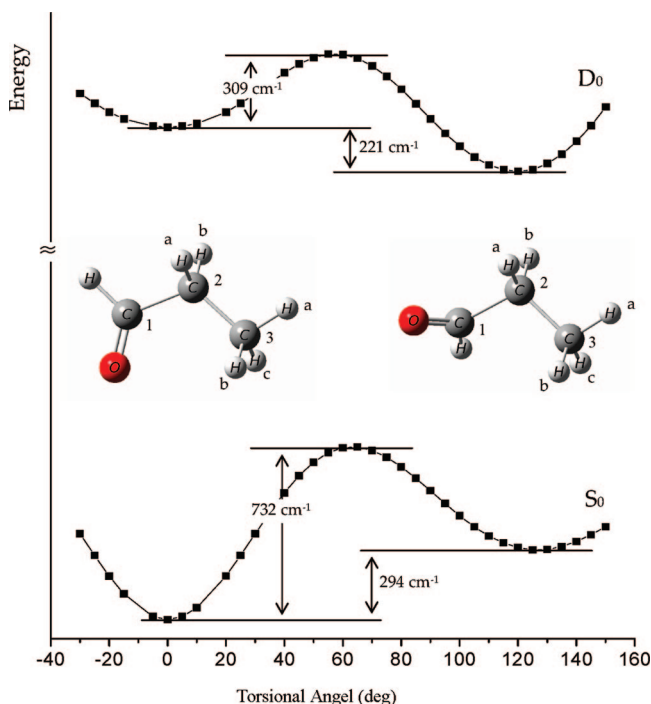


Figure 1. The DFT (B3LYP/6-311++G(d,p)) calculated potential energy curves of cis (left) and gauche (right) propanals along the conformational coordinate. The calculated IP difference of cis and gauche is 515 cm^{-1} , which is higher than the experimental value of 388 cm^{-1} (see the text).

then monitored as a function of the exciting VUV wavelength to give the MATI spectrum. All dye lasers, autotracker, and data taking processes were controlled by a personal computer. Calculations of molecular structures and normal modes were carried out at the MP2¹¹ or DFT^{12,13} level using the Gaussian 03W program package.¹⁴ Franck–Condon analysis was done based on the Duschinsky transformation method¹⁵ using a code developed by Peluso and co-workers.^{16,17} Natural bonding orbital (NBO) calculations were carried out at the MP2 level.

III. Results and Discussion

The conformational coordinate of propanal is along the dihedral angle between the plane containing C(1)=O and that of C(2)–C(3), resulting in the difference of the relative orientation of the C(1)=O group with respect to the C(3)H₃ group (Figure 1). The conformational preference of propanal has much been studied, and it is now widely accepted that the cis conformer is more stable than the gauche conformer in the neutral ground state. The density functional theory (DFT) calculation predicts that cis is about 0.84 kcal/mol more stable than gauche. From thermodynamics, the relative population of gauche is then estimated to be $\sim 20\%$, whereas that of cis should be $\sim 80\%$ at 300 K. The VUV MATI spectrum shows two distinct origin bands associated with cis and gauche propanals, giving the accurate IPs of $9.9997 \pm 0.0006 \text{ eV}$ and $9.9516 \pm 0.0006 \text{ eV}$, respectively, which are quite consistent with previously reported IP values⁸ (Figure 2). The relative intensity of the MATI origin of gauche located at $80\,265 \text{ cm}^{-1}$ is slightly more than 30% of that of the cis conformer at $80\,653 \text{ cm}^{-1}$. The interesting aspect of the experimental observation is that the propanal molecule does not undergo conformational cooling in the process of supersonic expansion with the carrier gas of He. In other words, the relative population of cis and gauche at 300 K seems to be maintained even in the supersonic jet where

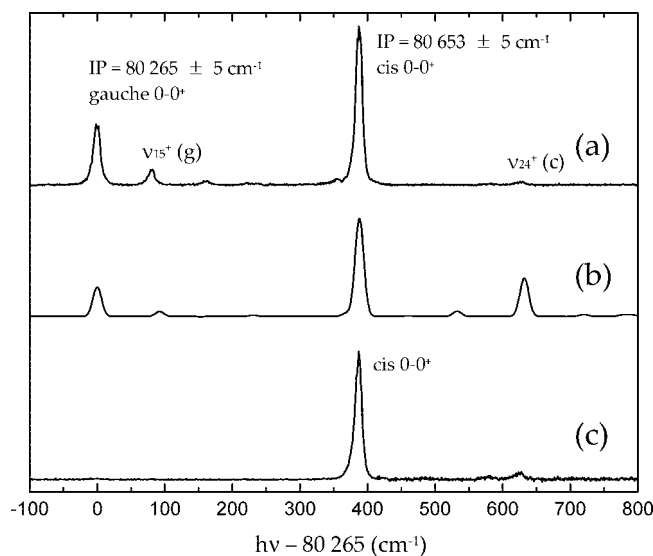


Figure 2. (a) The VUV-MATI spectrum of propanal expanded with He. (b) The simulation using the Franck–Condon analysis based on the DFT calculations. (c) The VUV-MATI spectrum of propanal supersonically cooled with Ar carrier gas at a backing pressure of 1 atm. In panel c, the gauche conformer is absent (see the text).

the final temperature of each conformational isomer is around 5 K. On the other hand, it should be noted that the conformational cooling becomes quite effective when Ar is being used as a carrier gas. Namely, when propanal is expanded with the Ar carrier gas, the MATI band due to the gauche propanal is completely vanished, whereas only that of cis is strongly observed (Figure 2). This is a very interesting observation and could be attributed to the different partial cross-sections of collisions with He or Ar depending on the vibrational mode of propanal. In general, the Ar carrier gas should be more effective in the momentum transfer per collision because of its heavier mass compared to He.¹⁸ Apparently it thus seems to be that the heavier and slower collision is more effective in the conformational cooling, although the detailed mechanism needs to be clarified.

The much higher IP of the cis propanal compared to that of gauche indicates that the conformational preference becomes reversed in the cationic ground state of propanal. Provided that the stabilization energy difference of cis and gauche in the neutral ground state is 0.84 kcal/mol, the gauche conformer is expected to be more stable by $\sim 0.63 \text{ kcal/mol}$ than the cis conformer in the cationic ground state (Figure 1). Since the origin bands of both conformational isomers are strongly observed in the VUV-MATI spectrum, the structural change upon ionization is not expected to be drastic. This implies that the nuclear layout of the gauche conformer is more favored for the charge delocalization compared to that of the cis conformer in the cationic ground state. The extent of the charge delocalization is closely related to the stabilization energy attributed to the hyperconjugation effect. NBO calculation at the MP2 level strongly supports the role of hyperconjugation in the stabilization of gauche in the cationic ground state. Namely, the delocalization energy of the cis conformer is calculated to be larger than that of the gauche conformer by 5.64 kcal/mol in the neutral ground state, while the delocalization energy in the cationic ground state is calculated to be larger for gauche than for cis by 7.53 kcal/mol.

The VUV-MATI spectroscopy provides direct information about the structural change that the molecule undergoes upon ionization. It is very intriguing, therefore, to investigate the

TABLE 1: Vibrational Frequencies of Cis and Gauche Propanals in the Neutral and Cationic Ground States (cm⁻¹)

| | | cis | | | gauche | | | | | |
|------------|-----|---------|--------|------|-------------------------|---------|------|------|-------------------------|-------------|
| | | neutral | cation | | neutral | cation | | | | |
| | | | calc | expt | description | neutral | calc | expt | description | |
| ν_1 | a' | 3106 | 3097 | | CH ₃ str. | a | 3104 | 3151 | CH ₂ str. | |
| ν_2 | | 3041 | 3005 | | CH ₃ str. | | 3101 | 3134 | CH ₃ str. | |
| ν_3 | | 3000 | 3000 | | CH ₂ str. | | 3082 | 3086 | CH ₃ str. | |
| ν_4 | | 2862 | 2819 | | C1H str. | | 3031 | 3018 | CH ₂ str. | |
| ν_5 | | 1804 | 1733 | | C=O str. | | 3008 | 2987 | CH ₃ str. | |
| ν_6 | | 1501 | 1489 | | CH ₃ deform. | | 2854 | 2889 | C1H str. | |
| ν_7 | | 1449 | 1417 | | CH ₂ deform. | | 1803 | 1734 | C=O str. | |
| ν_8 | | 1422 | 1389 | | CH ₃ deform. | | 1506 | 1488 | CH ₃ deform. | |
| ν_9 | | 1408 | 1280 | | CH ₂ wag. | | 1501 | 1446 | CH ₂ deform. | |
| ν_{10} | | 1363 | 1098 | | C1H rock. | | 1467 | 1409 | CH ₃ deform. | |
| ν_{11} | | 1107 | 1006 | | CH ₃ wag. | | 1422 | 1379 | CH ₃ deform. | |
| ν_{12} | | 1003 | 898 | | CH ₃ rock. | | 1410 | 1273 | CH ₂ wag. | |
| ν_{13} | | 846 | 586 | | C1C2 str. | | 1327 | 1221 | CH ₂ twist. | |
| ν_{14} | | 671 | 466 | | OCC bend. | | 1272 | 1147 | C1H rock. | |
| ν_{15} | | 252 | 245 | 240 | OCCC bend. | | 1157 | 1017 | CH ₂ twist. | |
| ν_{16} | a'' | 3110 | 3144 | | CH ₃ str. | | 1131 | 1010 | CH ₃ rock. | |
| ν_{17} | | 3020 | 3043 | | CH ₂ str. | | 1009 | 906 | CH ₃ rock. | |
| ν_{18} | | 1493 | 1420 | | CH ₃ deform. | | 920 | 860 | C1H deform. | |
| ν_{19} | | 1279 | 1240 | | CH ₂ twist. | | 875 | 792 | CH ₂ rock. | |
| ν_{20} | | 1144 | 1051 | | CH ₂ twist. | | 759 | 629 | C1C2 str. | |
| ν_{21} | | 905 | 864 | | C1H deform. | | 508 | 368 | OCC bend. | |
| ν_{22} | | 670 | 650 | | CH ₂ rock. | | 328 | 320 | CCC bend. | |
| ν_{23} | | 225 | 256 | | CH ₃ torsion | | 211 | 231 | CH ₃ torsion | |
| ν_{24} | | 131 | 72 | | CHO torsion | | 78 | 92 | 81 | CHO torsion |

conformer specificity in the ionization-driven structural change. Interestingly, the progression bands of which the fundamental frequency is 81 cm⁻¹ is found to be activated only for the gauche propanal (Figure 2). This band, according to the DFT calculation (Table 1), is associated with the torsional motion about the C(1)–C(2) bond, which corresponds to the conformational coordinate along which cis and gauche are separated by a certain barrier (Figure 1). This experimental fact, therefore, indicates that the gauche conformer, once ionized, undergoes a conformational change in order to be more stabilized. Meanwhile, the DFT calculations at the B3LYP level with the basis set of 6-311++G(d,p) support this experimental observation, and detailed geometrical parameters of each conformer are listed in Table 2. On the basis of the calculated geometry and vibrational frequencies, Franck–Condon analysis has been carried out for each conformer to simulate the corresponding MATI spectrum. The simulation matches with the experiment extremely well, as shown in Figure 2.

Even though the conformational change of gauche upon ionization is not drastic, it is intriguing to consider the driving force for this interesting conformer-specific movement of the molecule as it is ionized. The cis propanal does not undergo the structural change upon ionization along the conformational coordinate, even though its geometry in the cationic ground state is less favored in terms of the hyperconjugation compared to the gauche conformer ion. This suggests that the ionization-driven geometrical change of gauche along the conformational coordinate may not originate from the better hyperconjugation in the energy minimum structure. Rather, the steric effect caused by the valence electron repulsion could be mainly responsible for the torsional motion along the conformational coordinate. Namely, as the electron in the highest occupied molecular orbital (HOMO) is removed, the steric tension at the neutral gauche geometry is somewhat released to induce the conformational change. This makes sense if one notices that the HOMO is asymmetric with respect to the methyl moiety at the gauche geometry,

TABLE 2: Minimum Energy Structures of the Neutral and Cationic Ground States of Two Conformers of Propanal Calculated at the B3LYP Level with the Basis Set of 6-311++G(d,p). (Å, °)

| | cis | | gauche | |
|----------|---------|--------|---------|--------|
| | neutral | cation | neutral | cation |
| R(C1–O) | 1.206 | 1.183 | 1.206 | 1.185 |
| R(C1–H) | 1.113 | 1.117 | 1.114 | 1.111 |
| R(C1–C2) | 1.509 | 1.571 | 1.509 | 1.574 |
| R(C2–Ha) | 1.099 | 1.100 | 1.092 | 1.089 |
| R(C2–Hb) | | | 1.099 | 1.099 |
| R(C2–C3) | 1.527 | 1.509 | 1.537 | 1.524 |
| R(C3–Ha) | 1.093 | 1.098 | 1.092 | 1.100 |
| R(C3–Hb) | 1.092 | 1.090 | 1.093 | 1.091 |
| R(C3–Hc) | | | 1.094 | 1.090 |
| ∠C1C2C3 | 114.78 | 115.91 | 111.93 | 108.82 |
| ∠OC1C2 | 125.14 | 125.86 | 125.19 | 121.39 |
| ∠OC1C2C3 | 0.00 | 0.00 | 125.94 | 119.54 |

whereas it is symmetric at the cis geometry (Figure 3). In other words, since the HOMO at cis is symmetrically oriented with respect to the other valence electrons, the depletion of electron in the HOMO does not affect the steric repulsion as far as the geometry is concerned. Meanwhile, because of the asymmetric arrangement of the HOMO at the gauche geometry, the deficiency of electrons in the HOMO of the gauche propanal should give an unbalance of the steric repulsion with other valence electrons, resulting in the torsional motion along the conformational coordinate. This experimental fact suggests that the steric effect due to the valence electron repulsion may be significantly responsible for the relative instability of gauche in the neutral ground state. The asymmetric arrangement of valence electrons in the three-dimensional geometrical layout of gauche could also be responsible for the efficient conformational cooling of gauche into cis when Ar is used for the supersonic expansion (*vide supra*) since it may contribute to the increase of collisional cross section.

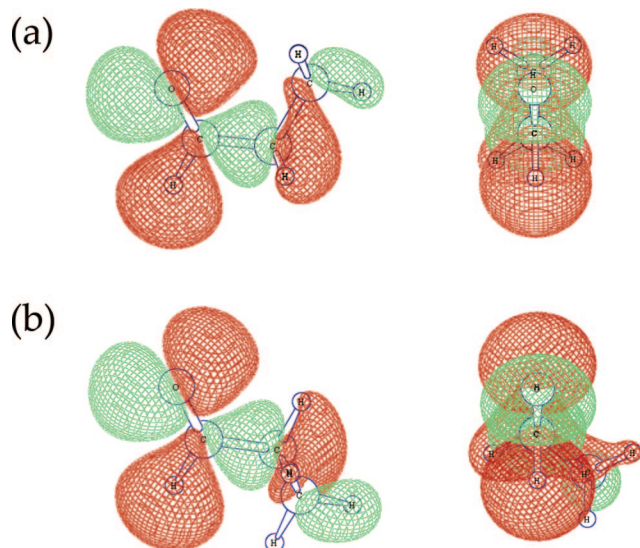


Figure 3. The HOMOs of (a) *cis*-propanal and (b) *gauche*-propanal. On the right, Newman projections are given.

IV. Summary and Conclusions

The *cis* and *gauche* conformational isomers of propanal have been investigated by VUV MATI spectroscopy. The ionization energy of each conformer has been most accurately and precisely measured. The *gauche* propanal, which is less stable compared to the *cis* propanal in the neutral ground state, is calculated to be more stable than *cis* in the cationic ground state. The more efficient charge delocalization at the *gauche* geometry compared to *cis* in the cationic ground state may be responsible for this observation. The MATI spectrum reflects the conformer-specificity in the ionization-driven structural change, providing the unique opportunity to investigate the role of the electron of the HOMO in the conformational preference. The torsional vibrational bands are found to be active only in the MATI spectrum of the *gauche* conformer ion, indicating that the *gauche* propanal undergoes a geometrical change upon ionization along the conformational coordinate. Asymmetric arrangement of the HOMO with respect to other valence orbitals at the *gauche* geometry seems to be the origin of the steric effect, especially in the neutral ground state. Hyperconjugation and steric effects are both responsible for any conformational preference, and the MATI spectroscopy is particularly useful since the role of

HOMO in those effects can be unambiguously investigated for each conformer separately.

Acknowledgment. This work was financially supported by KOSEF (R01-2007-000-10766-0 & M10703000936-07M0300-93610), the Echo Technopia 21 Project of KIRST (102-071-606), the Center for Space-Time Molecular Dynamics (R11-2007-012-01002-0), and the KISTI Supercomputing Center (KSC-2007-S00-1027).

References and Notes

- (1) McDonnell, C.; Lopez, O.; Murphy, P.; Bolaños, J. G. F.; Hazell, R.; Bols, M. *J. Am. Chem. Soc.* **2004**, *126*, 12374.
- (2) Sibi, M. P.; Stanley, L. M.; Nie, X.; Venkatraman, L.; Liu, M.; Jasperse, C. P. *J. Am. Chem. Soc.* **2006**, *129*, 395.
- (3) Gorenstein, D. G. *Chem. Rev.* **1994**, *94*, 1315.
- (4) Michalet, X.; Weiss, S.; Jäger, M. *Chem. Rev.* **2006**, *106*, 1785.
- (5) Park, S. T.; Kim, S. K.; Kim, M. S. *Nature* **2002**, *415*, 306.
- (6) Kim, M. H.; Shen, L.; Tao, H.; Martinez, T. J.; Suits, A. G. *Science* **2007**, *315*, 1561.
- (7) Choi, K.-W.; Ahn, D.-S.; Lee, J.-H.; Kim, S. K. *Chem. Commun.* **2007**, *10*, 1041.
- (8) Kim, M. H.; Shen, L.; Suits, A. G. *Phys. Chem. Chem. Phys.* **2006**, *8*, 2933.
- (9) Choi, S.; Choi, K.-W.; Kim, S. K.; Chung, S.; Lee, S. *J. Phys. Chem. A* **2006**, *110*, 13183.
- (10) Choi, K.-W.; Ahn, D.-S.; Lee, J.-H.; Kim, S. K. *J. Phys. Chem. A* **2006**, *110*, 2634.
- (11) Möller, C.; Plesset, M. S. *Phys. Rev.* **1934**, *46*, 618.
- (12) Becke, A. D. *J. Chem. Phys.* **1993**, *98*, 5648.
- (13) Lee, C.; Yang, W.; Parr, R. G. *Phys. Rev. B* **1988**, *37*, 785.
- (14) Frisch, M. J.; Trucks, G. W.; Schlegel, H. B.; Scuseria, G. E.; Robb, M. A.; Cheeseman, J. R.; Montgomery, J. A., Jr.; Vreven, T.; Kudin, K. N.; Burant, J. C.; Millam, J. M.; Iyengar, S. S.; Tomasi, J.; Barone, V.; Mennucci, B.; Cossi, M.; Scalmani, G.; Rega, N.; Petersson, G. A.; Nakatsuji, H.; Hada, M.; Ehara, M.; Toyota, K.; Fukuda, R.; Hasegawa, J.; Ishida, M.; Nakajima, T.; Honda, Y.; Kitao, O.; Nakai, H.; Klene, M.; Li, X.; Knox, J. E.; Hratchian, H. P.; Cross, J. B.; Bakken, V.; Adamo, C.; Jaramillo, J.; Gomperts, R.; Stratmann, R. E.; Yazyev, O.; Austin, A. J.; Cammi, R.; Pomelli, C.; Ochterski, J. W.; Ayala, P. Y.; Morokuma, K.; Voth, G. A.; Salvador, P.; Dannenberg, J. J.; Zakrzewski, V. G.; Dapprich, S.; Daniels, A. D.; Strain, M. C.; Farkas, O.; Malick, D. K.; Rabuck, A. D.; Raghavachari, K.; Foresman, J. B.; Ortiz, J. V.; Cui, Q.; Baboul, A. G.; Clifford, S.; Cioslowski, J.; Stefanov, B. B.; Liu, G.; Liashenko, A.; Piskorz, P.; Komaromi, I.; Martin, R. L.; Fox, D. J.; Keith, T.; Al-Laham, M. A.; Peng, C. Y.; Nanayakkara, A.; Challacombe, M.; Gill, P. M. W.; Johnson, B.; Chen, W.; Wong, M. W.; Gonzalez, C.; Pople, J. A. *Gaussian 03*, revision B.02; Gaussian: Wallingford, CT, 2003.
- (15) Duschinsky, F. *Acta Physicochim. USSR* **1937**, *7*, 551.
- (16) Peluso, A.; Santoro, F.; Re, G. D. *Int. J. Quantum Chem.* **1997**, *63*, 233.
- (17) Borrelli, R.; Peluso, A. *J. Chem. Phys.* **2003**, *119*, 8437.
- (18) Chou, C.-S.; Lin, K.-C. *J. Chem. Phys.* **1996**, *105*, 2719.

JP800775S